Investigation of Silicon Nitride Shadowed Selective Area Growth as an Enabling Technology for GaN Vertical Device Processing

Matthew M. Landi, Frank P. Kelly, Kyekyoon Kim

Department of Electrical and Computer Engineering, University of Illinois at Urbana-Champaign, Urbana, IL 61801, USA
e-mail: kevinkim@illinois.edu, Phone: +1-(217) 333-7162

Keywords: GaN, Selective Area Growth, Trench Sidewall Regrowth, Characterization, PAMBE

Abstract

Conventional processing routes for wide bandgap semiconductors such as SiC and GaN for power device applications are known to reduce device performance via the generation of high-leakage defects and deactivation of dopants. Here, the characterization of a novel masking method Silicon Nitride Shadowed, Selective Area Growth (SNS-SAG) is presented. The masks' ability to enable the growth of tall vertical features with smooth sidewalls, arrest and prevent the formation of screw dislocations, and resist in-diffusion of constituent masking materials is demonstrated via Cathodoluminescence (CL), Conductive Atomic Force Microscopy (C-AFM), and X-ray Photoelectron Spectroscopy (XPS).

INTRODUCTION

Techniques for the fabrication and processing of vertical power devices to date have fallen short of the quality standards of the present semiconductor market when applied to Gallium Nitride (GaN). GaN is a wide-bandgap semiconductor which can sustain extreme environments thermally, electrically, and chemically [1]. As such, GaN is an attractive material for power electronic devices. Advancements in halide vapor phase epitaxy have led to the development of high-quality bulk GaN substrates suitable for power device processing; consequently, fully vertical power devices can be realized [2]. GaN features grown on bulk substrates are often fabricated via planar growth by plasma assisted molecular beam epitaxy (PAMBE), or metal-organic chemical vapor deposition (MOCVD), with subsequent etching and ion-implantation. However, these methods are not without fault, namely, both ion-implantation and dry etching via inductively coupled plasma reactive ion etching (ICP-RIE) bombard the device area with high-energy ions. This bombardment reduces crystallinity, activation efficiency of incorporated dopant atoms, and furthermore, introduces irreparable damage to the sidewalls of the etched architectures structurally and electronically [3-8]. One cause for concern is the formation of screw and mixed type dislocations, as they are known leakage pathways and directly contribute to early reverse breakdown and an increase in leakage current in GaN power devices [9]. Although wet etching and annealing techniques have been explored to repair the bombard damage, no such technique to date has been capable of restoring the material to the as-grown state [10,11]. It is, apparent that to fully realize the potential of GaN, a method must be developed to generate device structures without intrinsic damage, and therefore, without the use of ion-implantation or ICP-RIE. In response, a masking technique compatible with PAMBE for SAG has been developed. A dual layer mask with under-etched Silicon Nitride foundation allows for the growth of smooth tall features with variable thickness. The key being a shadowing effect created by the SiO_2 capping layer, utilizing the line-of-sight nature of PAMBE growth. Nitrogen and Ga-vapor flux to the mask sidewall is restricted via the SiO_2, preventing polycrystalline GaN from nucleating on the sidewall there-by eliminating disruption of the selected growth regions. Further details on the development of the mask can be found in our sister paper. To ascertain the safety and efficacy of such a mask design, the grown architectures and processed wafers are characterized via XPS, CL, and C-AFM. Samples were grown via PAMBE on Al_2O_3 with AlN buffer layer and 5µm of n-type MOCVD GaN.

RESULTS AND DISCUSSION

During growth, the masked substrates rest at 800°C for 10^+ hours, sparking concern regarding in-diffusion of Si from the mask. Unintentional Si, being an n-type dopant in GaN, would pose an issue as in-diffusion could result in a multitude of issues including compensation of underlying p-doped layers, formation of n-type wells where there should otherwise not be, and potential development of additional p-n junctions. To explore these concerns, XPS spectra were obtained on a Kratos Axis Ultra with a monochromatic Al X-ray source. Analysis of the binding energies reveals that no Si is incorporated into the substrate during the growth process from the SNS-SAG mask, as shown in Figure 1. The solid lines trace the binding energies of the Ga associated peaks, while the dashed lines trace the binding energies of Si. Neither the Si 2p (100eV) nor 2s (151eV) peak is apparent from the high-resolution scan [12]. Furthermore, XPS shows no contamination other than a small carbon peak from IPA residue. While here it is shown that the performance of GaN devices grown via SNS-SAG will not be hindered by unintentional Si diffusion, attention now turns to the quality of the regrown architectures.

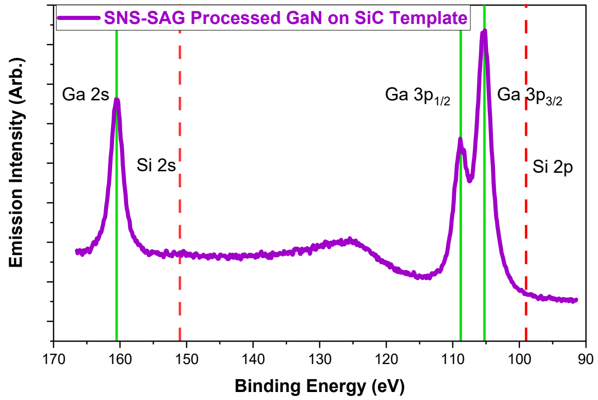

Fig. 1. X-ray spectrum of GaN surface after SNS-SAG processing. Dashed lines trace Si binding energies, while the solid lines trace Ga binding energies.

To locate potential deep center electronically active defects and screw dislocations within the regrowth, CL and C-AFM techniques were employed [9,13]. Secondary electron and CL images were taken on a JEOL 7000F with 5kV accelerating voltage to isolate the grown film and sidewall surface from any potential template effects. A CL spectrum of an isolated mesa and sidewall is shown below in Figure 2. The primary peak at 3.4eV corresponds to the GaN bandgap; the secondary peak is related to the second order diffraction artifact of the primary peak. Deep center states are generally attributed to a combination of shallow donors, double donor levels, or deep acceptor levels [14]. Their presence is indicated by a sub-bandgap transition within the yellow or blue line range (2-3eV) [14,15]. As seen in Figure 2, these peaks are absent in this work, suggesting an absence of deep center electrically active states.

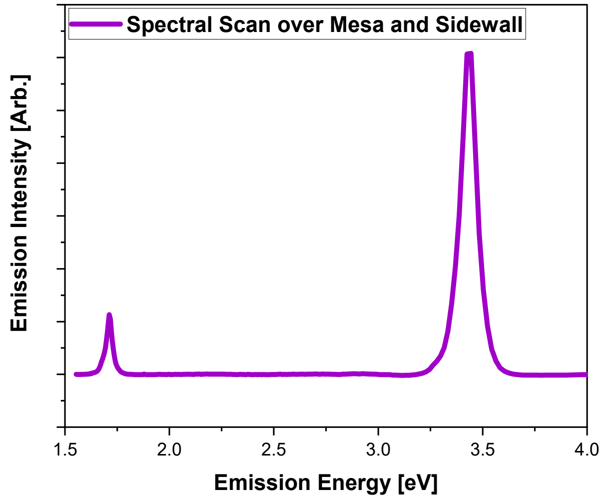

Fig. 2. CL spectrum of SNS-SAG processed mesa architectures. The prominent peak at 3.4eV is associated with the GaN bandgap. The 2nd order diffraction artifact is visible at 1.7eV.

The 360nm mono-CL image shown in Figure 3(a) exhibits uniform emission along the sidewall (with high intensity due to edge effects), mesa, and substrate. Due to the electron channeling nature of screw dislocations, these defects would appear as glaring dark circles in the CL image, as the excited electrons in this region are swept away along the dislocation line rather than recombined with holes with emission [13]. Deep level defects unrelated to screw or mixed typed dislocation centers are also known to appear as dark features in CL scans as the dark regions correspond to a locally high probability of non-radiative recombination [13]. These features are not seen in this work. Figure 3(b) shows the secondary electron image of the sidewall shown in Figure 3(a). Figure 3(c) is a secondary electron image illustrating tightly spaced SNS-SAG architectures with no loss in sidewall quality; this capability of the SNS-SAG mask to resolve fine features will be necessary for expansion into complex devices such as trench gate field effect transistors.

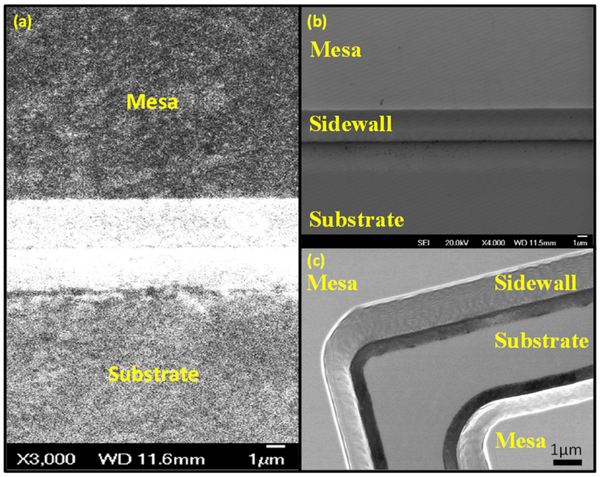

Fig. 3. (a) Mono-CL 360nm plan-view image of GaN substrate, mesa, and sidewall. (b) Corresponding Secondary electron image (a). (c) Secondary electron image of tightly spaced SNS-SAG grown mesas(a).

Finally, AFM was utilized to locate areas of high current density and ascertain the quality of the mesa sidewall. Proper electrical contact for side-by-side features in GaN devices fabricated via SNS-SAG regrowth requires smooth interfaces, thus the surface roughness is of interest when considering intricate devices structures with multiple masking and regrowth processes. To obtain reliable RMS values, and to avoid crashing the side of the AFM tip into the sidewall itself, a custom chuck was designed at a 30-degree tilt to hold the regrown samples as shown in Figure 4(d). The sample was situated such that the edge of the regrown region was ‘floating’ off the chuck. The tip was then lowered to the sample edge where the measurement could take place approximately normal to the sidewall surface. A schematic of the set-up is shown in Figure 4(d). Measurements were taken on an Asylum Cypher MFP-3D. Tapping mode AFM scans shown in Figure 4(a) reveal a mesa RMS roughness of 0.098nm over a 1µm scan, and 0.112nm over a 5µm scan, for undoped GaN. GaN mesas grown with a 500nm Mg-doped capping layer exhibit 0.223nm roughness for a 1µm scan, and 0.332nm for a 5µm scan size as shown in Figure 4(c). Mg concentration in the capping layer was 7.9x10^{19}cm^{-3}. Figure 4(b) shows a contact mode AFM scan of a mesa sidewall with the corresponding C-AFM signal which is overlaid. Regions of locally high current are shown in white and outlined.

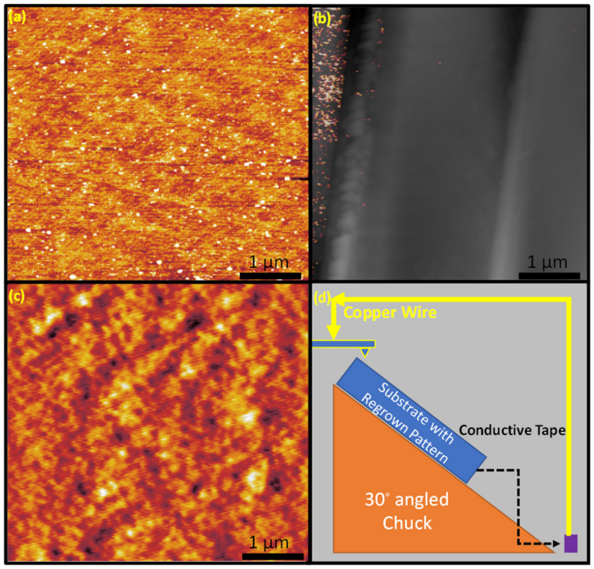

Fig. 4. (a) AFM scan of undoped PAMBE SNS-SAG mesa, RMS roughness of 0.098nm over 1µm^2 scan. (b) Contact mode topography AFM scan (greyscale) overlaid with the C-AFM current scan (orange). (c) AFM scan of Mg-doped PAMBE SNS-SAG mesa, RMS roughness of 0.223nm over 1µm^2 scan. (d) Experimental set-up illustrating the effect of the tilted stage and the resulting side-wall normal orientation of the AFM probe.

We do not note any regions of locally high conductivity along the sidewall or mesa from the C-AFM measurements, rather, the only conductive region is the n-type GaN substrate as seen from the left-hand side of Figure 4(b). The RMS roughness calculated along the sidewall ranges from 0.5nm-5nm over a 1µm scan size in preliminary samples. This roughness is highly promising and can be improved with further mask optimization. Lack of local conduction in C-AFM scans in combination with the absence of regions of locally high non-radiative recombination in CL scans supports the claim that the SNS-SAG mask enables growth of high-quality GaN mesas which resist the formation and propagation of screw type defects under proper growth conditions. Furthermore, CL and XPS reveal that the mask is safe to use in GaN processing and does not contaminate the substrate or regrown regions.

Preliminary SNS-SAG processed Schottky devices show four orders of magnitude improvement in leakage current over equivalent design ICP-RIE processed devices [16]. This demonstrates the practical advantages of using SNS-SAG processing for power electronic devices, and stands as a launching point for improvements in mask quality, and extension to sophisticated architectures and new materials.

CONCLUSIONS

GaN vertical architectures grown via a novel growth masking method SNS-SAG are characterized via XPS, CL, and C-AFM to determine the viability of SNS-SAG (patent pending) as an enabling technology for GaN vertical device processing. XPS and CL measurements show no sign of in-diffusion of Si from the mask. CL and C-AFM together indicate that the sidewalls and mesa resist the propagation and formation of screw dislocations. This suggests that the SNS-SAG mask is effective and advantageous for use in GaN vertical processing for high-efficiency high-power devices.

ACKNOWLEDGEMENTS

This work was supported by the Office of Naval Research Award N00014-21-1-2544 (PM: Lynn Petersen). Data was collected at the Frederick Seitz Materials Research Laboratory. The authors would like to thank Dr. Haasch, Dr. Chen, and Dr. Walsh for their assistance in data collection.

REFERENCES

[1] T. J. Anderson et at. *Electron Lett*., vol. 50, no. 3, pp. 197-198, 2014.
[2] Karolina Grabianska et al. *Electronics,* vol. 9, 1342, 2020
[3] H. Cho et al. *J. Phys. D: Appl. Phys.*, vol. 41, 155314, 2008.
[4] Y. Zhang et al., *IEEE Trans. Electron Devices*, vol. 62, 2155, 2015.
[5] T. Hayashida et al. *Appl. Phys. Exp.*, vol. 10, 061003, 2017.
[6] B. J. Pong et al. *J. Appl. Phys.*, vol. 83, 5992, 1998.
[7] J. Chen et al. *Appl. Phys. Exp.*, vol. 12, 051010, 2019.
[8] T. J. Anderson et al. *IEEE Trans. Semicond. Manuf*., vol. 29, no.4, pp. 342-348, 2016.
[9] S. Besendorfer et al. *Journal of Applied Physics*, vol. 127, 015701, 2020
[10] H. Kim, *Electronics Letters.*, vol. 44, no. 17, 2008.
[11] J. D. Greenlee et al. *ECS Journal of Solid State Science and Technology*, vol. 4, pp. 382-386, 2015.
[12] J.F. Moulder et al. "Handbook of X-Ray Photoelectron Spectroscopy" Minnesota, Perkin-Elmer Corporation, 1992.
[13] J. Wang et al. *Superlattices and Microstructures,* vol. 99, pp. 77-82, 8278, 2016.
[14] M. A. Reshchikov, *Nature Scientific Reports,* vol. 8, no. 8091, 2018
[15] T. Suski et al. *Applied Physics Letters,* vol. 67, no. 2188, (1995)
[16] P. Sarker et al., *IEEE Journal of the Electron Devices Society*, vol. 9, pp. 68-78, 2021.

ACRONYMS

SNS-SAG: Silicon Nitride Shadowed Selective Area Growth
PAMBE: Plasma-Assisted Molecular Beam Epitaxy
MOCVD: Metal Organic Chemical Vapor Deposition
XPS: X-ray Photoelectron Spectroscopy
CL: Cathodoluminescence
C-AFM: Conductive Atomic Force Microscopy
ICP-RIE: Inductively Coupled Plasma, Reactive Ion Etching
SE: Secondary Electron